Spin-2 $N\Omega$ Dibaryon from Lattice QCD

Faisal Etminan[a,b,c], Hidekatsu Nemura[a], Sinya Aoki[a,c], Takumi Doi[d], Tetsuo Hatsuda[d,e], Yoichi Ikeda[d], Takashi Inoue[f], Noriyoshi Ishii[a], Keiko Murano[c], Kenji Sasaki[a], (HAL QCD Collaboration)

[a] *Center for Computational Sciences, University of Tsukuba, Ibaraki 305-8571, Japan*
[b] *Department of Physics, Faculty of Sciences, University of Birjand ,Birjand 97175-615, Iran*
[c] *Yukawa Institute for Theoretical Physics, Kyoto University, Kyoto 606-8502, Japan*
[d] *Theoretical Research Division, Nishina Center, RIKEN, Saitama 351-0198, Japan*
[e] *Kavli IPMU (WPI), The University of Tokyo, Chiba 277-8583, Japan*
[f] *Nihon University, College of Bioresource Sciences, Kanagawa 252-0880, Japan*

Abstract

We investigate properties of the N(nucleon)-Ω(Omega) interaction in lattice QCD to seek for possible dibaryon states in the strangeness -3 channel. We calculate the $N\Omega$ potential through the equal-time Nambu-Bethe-Salpeter wave function in 2+1 flavor lattice QCD with the renormalization group improved Iwasaki gauge action and the nonperturbatively $\mathcal{O}(a)$ improved Wilson quark action at the lattice spacing $a \simeq 0.12$ fm on a $(1.9 \text{ fm})^3 \times 3.8$ fm lattice. The ud and s quark masses in our study correspond to $m_\pi = 875(1)$ MeV and $m_K = 916(1)$ MeV. At these parameter values, the central potential in the S-wave with the spin 2 shows attractions at all distances. By solving the Schrödinger equation with this potential, we find one bound state whose binding energy is $18.9(5.0)(^{+12.1}_{-1.8})$ MeV, where the first error is the statistical one, while the second represents the systematic error.

Keywords:
$N\Omega$ interaction, $N\Omega$ potential, $N\Omega$ dibaryon, Lattice QCD

1. Introduction

Possible existence of strange dibaryons is one of the long standing problems in hadron physics. Among others, the H dibaryon ($uuddss$) with $J^P = 0^+$ and I(isospin)=0 [1], and the $N\Omega$ dibaryon ($uudsss$ or $uddsss$) with $J^P = 2^+$ and I=1/2 [2], are the most interesting candidates. Since the

Pauli exclusion principle does not operate among quarks in these systems, they can in principle be compact six-quark states unlike the deuteron [3, 4].

Experimentally, if the mass of the H dibaryon is close to $2m_\Lambda = 2231$ MeV, its strong-decay width is suppressed, so that it may appear as a sharp resonance. Similarly, if the spin-2 $N\Omega$ dibaryon is a S-wave bound state of N and Ω, the strong decays to octet-decuplet systems are prohibited kinematically [1] and those into octet-octet systems (e.g. $\Lambda\Xi$) are suppressed dynamically due to the D-wave nature. Therefore, the spin-2 $N\Omega$ dibaryon, if it is a bound state or a sharp resonance, could be observed e.g. by relativistic heavy-ion collisions at RHIC and LHC, or by the hadron beam experiments at J-PARC and FAIR.

Although numerous attempts have been done to estimate the binding energy of strange dibaryon states in QCD motivated models, results were highly dependent on the model assumptions. Only recently, first principle calculations based on lattice QCD became available for multi hadrons due to the development of advanced techniques such as the Lüscher's method [5] and the HAL QCD method [6, 7, 8, 9, 10]. In particular, the H-dibaryon from the point of view of baryon-baryon interactions was first studied by 3-flavor QCD simulations in [11], and a possible shallow bound state in the flavor-SU(3) limit was suggested. Such a possibility was later explored and confirmed by more extensive simulations with relatively heavy quark masses in 2+1 flavor QCD [12] and in 3 flavor QCD [13, 14]. The fate of H in the real world, however, is still uncertain [15, 14, 16] and needs to be investigated further.

In this paper, by using (2+1)-flavor lattice QCD simulations with the HAL QCD method (reviewed in [10]), we carry out an exploratory study of the spin-2 $N\Omega$ dibaryon. Our strategy is to derive a potential between N and Ω in the ${}^5S_2$ channel[2] (S-wave and spin-2) from the Nambu-Bethe-Salpeter (NBS) wave function measured on the lattice. Although the potential itself is not a direct physical observable, it is a useful tool to derive various physical quantities such as the binding energy and the phase shift (see the review

[1] Note that the ordering of the thresholds in the octet-decuplet and decuplet-decuplet systems with strangeness=-3 and charge=0 reads $P\Omega^-(2611\text{MeV}) < \Lambda\Xi^{0*}(2648\text{MeV}) < \Xi^0\Sigma^{0*}(2699\text{MeV}) < \Xi^-\Sigma^{+*}(2705\text{MeV}) < \Sigma^0\Xi^{0*}(2724\text{MeV}) \sim \Sigma^+\Xi^{-*}(2724\text{MeV}) < \Sigma^{0*}\Xi^{0*}(2916\text{MeV}) < \Sigma^{+*}\Xi^{-*}(2918\text{MeV})$.

[2] We use the standard notation ${}^{2S+1}L_J$ in the continuous space to specify quantum numbers.

[10] for details). For relatively heavy u and d quark masses corresponding to $m_\pi = 875$ MeV and $m_K = 916$ MeV, we find that the $N\Omega$ system has one bound state with the binding energy ($B_{N\Omega}$) of about 19 MeV with the statistical error of 5 MeV. Since $B_{N\Omega}$ obtained in quark models ranges from negative value (resonance) to $\mathcal{O}(100)$ MeV (deeply bound state) [17, 18], our exploratory investigations would give useful information to both theoretical and experimental studies on the $N\Omega$ dibaryon.

2. Basic formulation

We define the $N\Omega$ potential at low-energies through the equal-time NBS wave function $\phi(\vec{r})$ which satisfies the Schrödinger-type equation at low energies,

$$-\frac{1}{2\mu}\nabla^2\phi(\vec{r}) + \int U(\vec{r},\vec{r'})\phi(\vec{r'})d^3\vec{r'} = E\phi(\vec{r}). \tag{1}$$

Here $\mu = m_N m_\Omega/(m_N + m_\Omega)$ is the reduced mass of the $N\Omega$ system, and $E \equiv k^2/(2\mu)$ is the kinetic energy in the center-of-mass frame. It is important to note that the nonlocal potential $U(\vec{r},\vec{r'})$ does not depend on k [8]. At low energies, we expand the nonlocal potential in terms of the relative velocity as[19] $U(\vec{r},\vec{r'}) = V_{N\Omega}(\vec{r},\vec{\nabla})\delta(\vec{r}-\vec{r'})$.

The equal-time NBS wave function in the S-wave is obtained as

$$\begin{aligned}
\phi(r) &= \frac{1}{24L^3}\sum_{\mathcal{R}\in O}\sum_{\vec{x}} P^S_{\alpha\beta,\ell}\left\langle 0\left|N_\alpha(\mathcal{R}\left[\vec{r}\right]+\vec{x},t)\Omega_{\beta,\ell}(\vec{x},t)\right|N\Omega;W\right\rangle, \qquad (2)\\
N_\alpha(x) &= \varepsilon_{abc}(u^a(x)C\gamma_5 d^b(x))q^c_\alpha(x), \quad \Omega_{\beta,\ell}(x) = \varepsilon_{abc}s^a_\beta(x)(s^b(x)C\gamma_l s^c(x)),
\end{aligned}$$

where $W = \sqrt{k^2+m_N^2}+\sqrt{k^2+m_\Omega^2}$ is the total energy, α and β denote Dirac indices, l is a spatial vector index of the gamma matrix γ_l, the color indices are given by a, b, c , and $C = \gamma_4\gamma_2$ is the charge conjugation matrix. Here N corresponds to a proton (neutron) for $q = u(d)$. The summation over $\mathcal{R} \in O$ is taken for all cubic-group elements to project out the S-wave [3]. The summation over $\vec{x}$ is taken to project out the state with zero total-momentum. We take local interpolating operators $N_\alpha(x)$ and $\Omega_{\beta,\ell}(y)$ for the nucleon and Ω: Although the potential depends on the choice of these

[3]Due to the periodic boundary condition, this projection cannot remove the higher orbital components with $L \geq 4$, which however are expected to be small at low energies.

operators, observables do not depend on the choice [8]. Projection operators ($P^{S=2}_{\alpha\beta,\ell}$) are used to select the spin 2 state. It is important to note that the NBS wave function at asymptotically large $|\vec{r}|$ carries full information of the phases of the S-matrix [20, 21, 22, 23].

On the lattice, the NBS wave function is extracted from the 4-point function as

$$\begin{aligned} F_{N\Omega}(\vec{x}-\vec{y},t-t_0) &= \left\langle 0 \left| N_\alpha(\vec{x},t)\Omega_{\beta,\ell}(\vec{y},t)\overline{J}_{N\Omega}(t_0) \right| 0 \right\rangle \\ &\simeq \sum_n A_n \left\langle 0 \left| N_\alpha(\vec{x},0)\Omega_{\beta,\ell}(\vec{y},0) \right| N\Omega;W_n \right\rangle e^{-W_n(t-t_0)}, \\ A_n &= \left\langle N\Omega;W_n \left| \overline{J}_{N\Omega}(t=0) \right| 0 \right\rangle \end{aligned} \tag{3}$$

where $\overline{J}_{N\Omega}(t_0)$ is a wall-source operator located at t_0, and $|N\Omega;W_n\rangle$ is an eigenstate with an eigen-energy W_n. For $t-t_0 \gg 1$, $F_{N\Omega}$ is dominated by the lowest energy eigenstate.

In the present paper, we consider the single channel scattering in the S-wave and consider the effective central potential obtained as a leading order term of the velocity expansion: $V_C(r) = \frac{1}{2\mu}\frac{\nabla^2\phi(r)}{\phi(r)} + E$. As shown in Ref. [9], such a potential can be obtained most efficiently by the time-dependent HAL QCD method, which does not require the difficult task to separate each scattering state:

$$V_C(r) \simeq \frac{1}{2\mu}\nabla^2 R(r,t)/R(r,t) - \frac{\partial}{\partial t}\log R(r,t), \tag{4}$$

where $R(r,t) = F_{N\Omega}(r,t)/e^{-(m_N+m_\Omega)t}$ with $F_{N\Omega}(r,t)$ being obtained from $F_{N\Omega}(\vec{r},t)$ by the S-wave projection. In the above equation, we have assumed that relativistic corrections $\left(\frac{\partial_t^2}{m_{N,\Omega}}\right)\left(\frac{\partial_t}{m_{N,\Omega}}\right)^n$ with $n \geq 0$ are small. (For the NN system in the elastic region, such corrections have been shown to be very small [9].)

3. Numerical results

We employ 700 gauge configurations generated by CP-PACS and JLQCD Collaborations[24] with the renormalization group improved Iwasaki gauge action and the nonperturbatively $\mathcal{O}(a)$ improved Wilson quark action[25] at $\beta = 1.83$ ($a \simeq 0.12$ fm) on the $16^3 \times 32$ lattice. The Dirichlet (periodic) boundary condition is imposed for quarks in the temporal (spatial) direction.

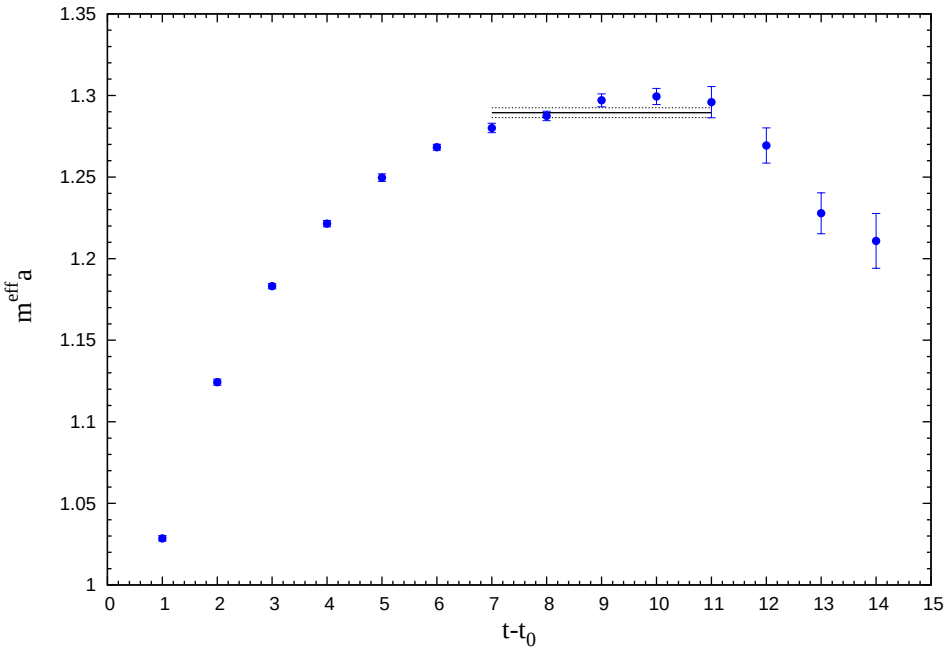

Figure 1: Effective mass of Ω as a function of $t - t_0$. The solid line represents the central value in the fit range $t-t_0 = 7-11$, while the dashed lines show the statistical uncertainty of the effective mass.

The wall source is used with the Coulomb gauge fixing, while the sink operator is projected to the A_1^+ representation of the cubic group, so that the NBS wave function is dominated by the S-wave component. A number of sources per configuration is 8. Statistical errors in this report are estimated by the Jack-Knife method with a bin size of 100 configurations, though errors do not change much as long as the bin size is larger than 10 configurations. The hopping parameters in our calculation are $(\kappa_{ud}, \kappa_s) = (0.13760, 0.13710)$, and the corresponding hadron masses obtained with 32 sources was given in Table 4 (Set 1) of Ref. [10]: $m_N = 1806(3)$ MeV, $m_\Lambda = 1835(3)$ MeV and $m_\Xi = 1867(2)$ MeV. In addition, we use $m_\Omega = 2105(5)$ MeV for our study, calculated from 8 sources with the fitting range $t-t_0 = 7-11$, whose effective mass is shown in Fig.1.

The S-wave $N\Omega$ system with spin 2 can decay into the D-wave $\Lambda\Xi$ system in the real world, though such coupling is expected to be suppressed kinematically. On our lattice setup with relatively heavy quarks, such a D-

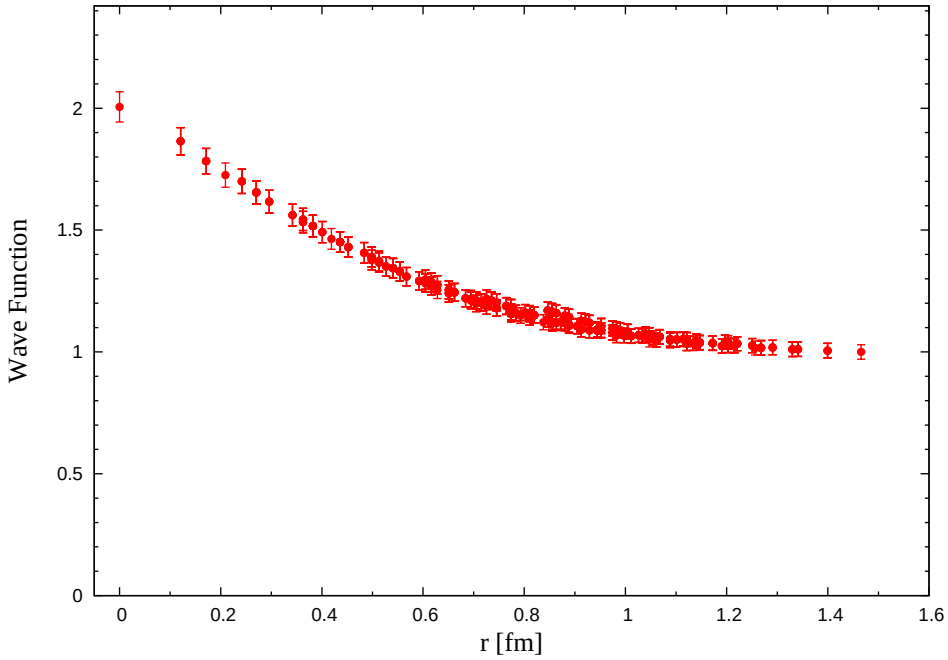

Figure 2: The NBS wave function for $N\Omega$ in the ${}^5S_2$ channel at $t - t_0 = 8$. The wave function is normalized to 1 at the maximum distance by multiplying an overall factor. Only statistical errors are shown.

wave threshold is located at $W_{\rm min} = \sqrt{m_\Lambda^2 + p_{\rm min}^2} + \sqrt{m_\Xi^2 + p_{\rm min}^2} \simeq 3920$ MeV for $p_{\rm min} = 2\pi/L \simeq 645$ MeV. This is slightly above $m_N + m_\Omega \simeq 1806 + 2105 = 3911$ MeV, so that we focus only on the $N\Omega$ channel in this report. More sophisticated analysis using the coupled-channel HAL QCD method [26, 27, 23, 28] is left for future studies.

Let us first show the $N\Omega$ NBS wave function in Fig. 2 as a function of the relative distance r in the ${}^5S_2$ channel at $t - t_0 = 8$. The wave function is normalized to 1 at the maximum distance by multiplying an overall factor, which does not affect the potential and observables. The NBS wave function increases as the distance decreases, suggesting the attractive interaction between N and Ω.

In Fig. 3, we show the $N\Omega$ effective central potential $V_C(r)$ in the ${}^5S_2$ channel at $t - t_0 = 8$; the first and the second terms in Eq. (4) are separately shown by green square and blue triangle points, respectively, together with

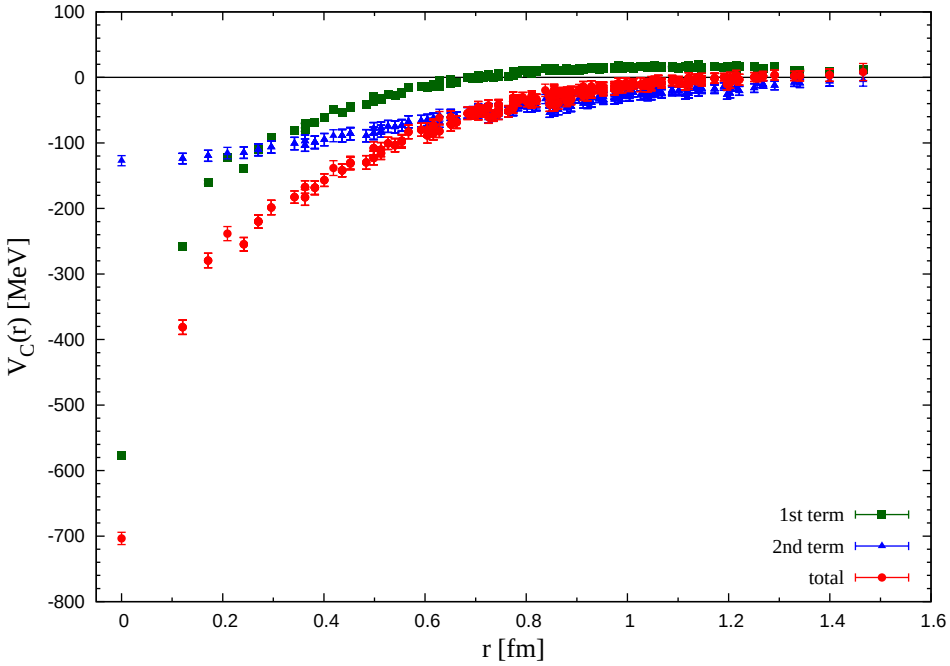

Figure 3: The effective central potential $V_C(r)$ (red circles) for $N\Omega$ in the ${}^5S_2$ at $t-t_0 = 8$, together with its breakup, the first (green squares) and the second (blue triangles) terms in Eq. (4). Only statistical errors are shown.

the total potential $V_C(r)$ shown by the red circle points. Note that the second term in Eq. (4) is essential to extract potentials reliably from 4-pt functions even in the presence of excited state contributions[9]. We find that $V_C(r)$ in Fig. 3 is attractive at all distances as expected from the behavior of the NBS wave function in Fig. 2.

Important observation emphasized in [9] is that the ground state saturation ($t \gg t_0$) is not necessary in our formulation and one can extract the non-local potential by using the information from finite $t - t_0$ as long as the inelastic threshold does not couple strongly. Furthermore, one can check the validity of the velocity expansion by looking at the t-dependence of the resultant local potentials. In Fig. 4, we compare $V_C(r)$ for $t - t_0 = 7 \sim 9$: Since they are consistent with each other within the error bars for all r, we conclude that the velocity expansion is working well for the low-energy scattering between N and Ω.

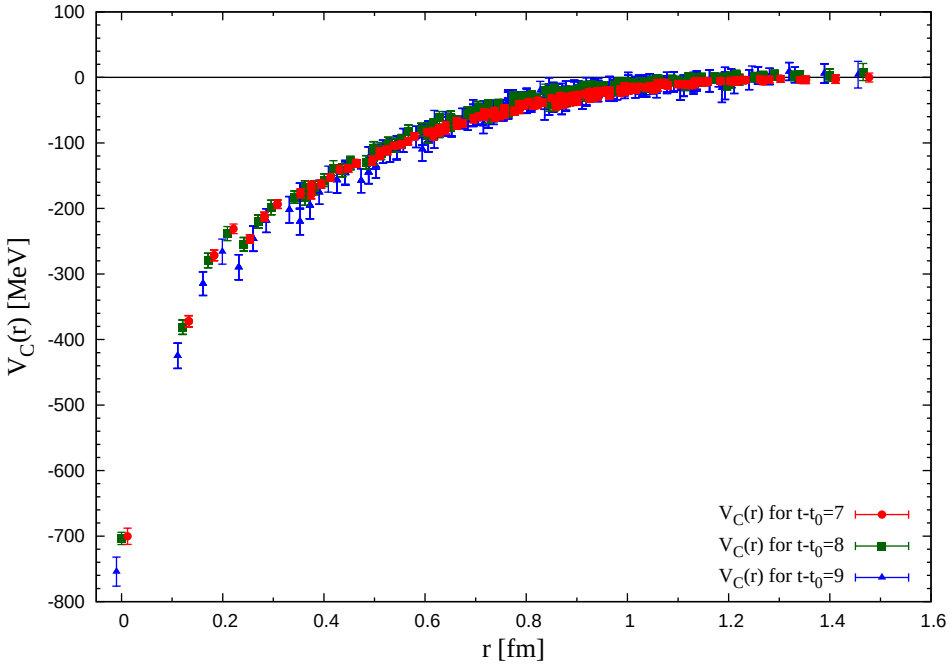

Figure 4: A comparison of the effective central potential $V_C(r)$ for $N\Omega$ in the ${}^5S_2$ at $t-t_0 = 7$ (red circles), 8 (green squares) and 9 (blue triangles). For visibility, data are a little shifted horizontally at each $t-t_0$. Only statistical errors are shown.

4. Scattering phase shift and binding energy

In order to calculate the $N\Omega$ scattering phase shift from the potential obtained in the previous section, we fit $V_C(r)$ with the Gaussian + (Yukawa)^2 form adopted in our previous analysis of the H-dibaryon in lattice QCD[13]:

$$V_C(r) = b_1 e^{-b_2 r^2} + b_3 (1 - e^{-b_4 r^2})^n (e^{-b_5 r}/r)^2, \tag{5}$$

where we take either $n = 2$ (the same form as [13]) or $n = 1$. Fitted results for the potential at $t - t_0 = 8$ are shown in Fig. 5 by a solid dark-green (dotted blue) line for $n = 1$ ($n = 2$) with χ^2/d.o.f. =0.95 (0.93).

Using the fitted potential $V_C(r)$, we solve the Schrödinger equation in the infinite volume to calculate the $N\Omega$ scattering phase shift in the ${}^5S_2$ channel. Fig. 6 shows the scattering phase shift $\delta(E)$ extracted from the potential at $t - t_0 = 8$ with $n = 1$, as a function of the kinetic energy $E = k^2/(2\mu)$ in the center of mass frame. (The results for $n = 2$ gives negligible difference from

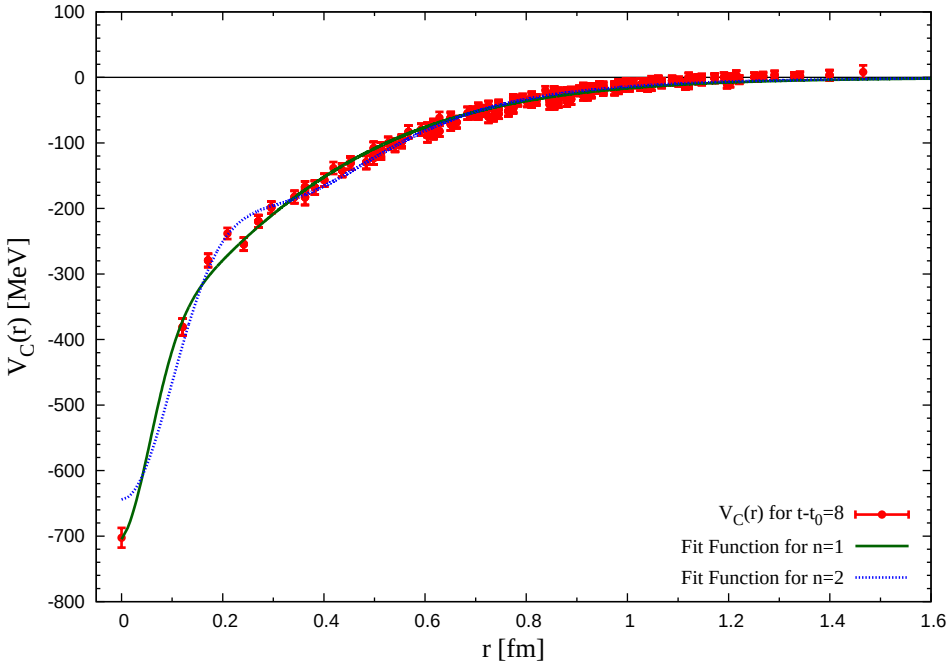

Figure 5: Fit of the effective central potential $V_C(r)$ at $t-t_0 = 8$ for $n = 1$ (solid dark-green line) and for $n = 2$ (dotted blue line). only statistical errors are shown.

those for $n = 1$ compared to the statistical errors.) Note that systematic errors associated with the leading order approximation V in the velocity expansion for the non-local potential U may become more sizable at larger kinetic energies.

The scattering phase shift becomes 180 degrees at $E = 0$ and rapidly decreases as E increases, which implies the existence of a bound state in this channel. We thus calculate the binding energy B, which is given in Table 1 at each $t - t_0$ with $n = 1$ and 2, together with the scattering length a and the effective range r_e, where the scattering length and the effective range are defined from the scattering phase shift $\delta(E)$ as

$$k \cot \delta(E) \quad = \quad \frac{1}{a} + \frac{r_e}{2} k^2 + O(k^4). \tag{6}$$

Since effective masses of both N and Ω show plateau for $t - t_0 \geq 7$, the central value and statistical error of the observables are estimated from the weighted average over $8 \leq t - t_0 \leq 11$ with $n = 1$. To estimate the

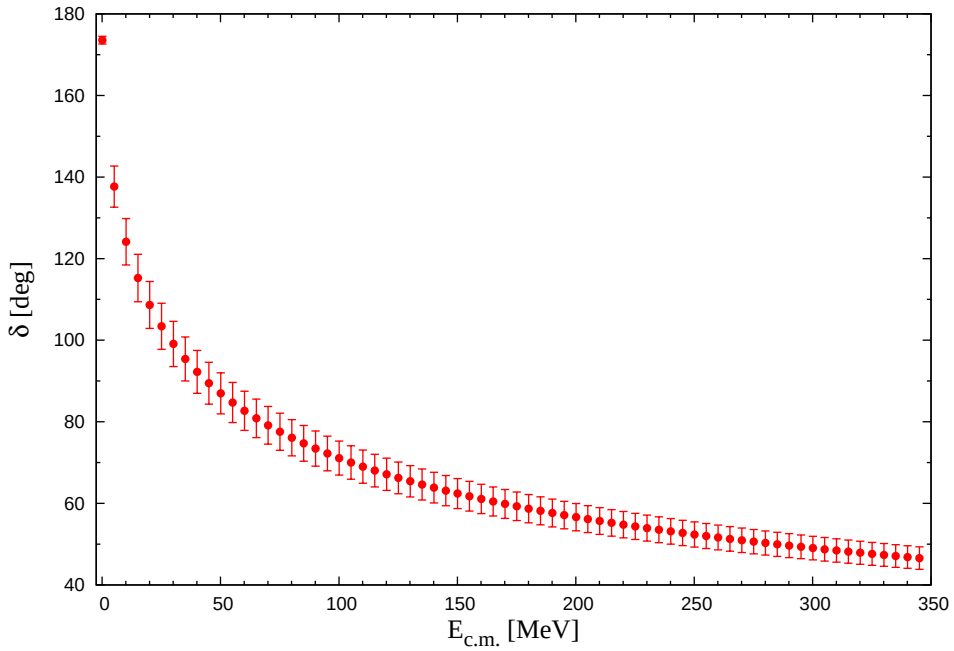

Figure 6: Scattering phase shift δ as a function of the kinetic energy $E = k^2/(2\mu)$ in the center of mass frame, obtained from the potential with the $n = 1$ fit at $t - t_0 = 8$. Only statistical errors are shown.

systematic errors, we consider the observables obtained from the average over $7 \le t - t_0 \le 11$ and over $9 \le t - t_0 \le 11$, as well as those from the average over $t_{\rm min} \le t - t_0 \le 11$ ($t_{\rm min} = 7, 8, 9$) with $n = 2$. Finally we obtain

$$B_{N\Omega} = 18.9(5.0)(^{+12.1}_{-1.8})\ \text{MeV}, \quad (7)$$

$$a_{N\Omega} = -1.28(0.13)(^{+0.14}_{-0.15})\ \text{fm}, \quad (8)$$

$$(r_e)_{N\Omega} = 0.499(0.026)(^{+0.029}_{-0.048})\ \text{fm}. \quad (9)$$

Here the numbers in the first parenthesis correspond to the statistical error, while those in the second parenthesis show the systematic errors obtained by taking the largest difference between the central value and the other 5 values. Note that this systematic uncertainty is still sizable, in particular for the binding energy.

Table 1: The binding energy, the scattering length and the effective range obtained from each potential at $t - t_0$ with $n = 1, 2$.

n	$t - t_0$	B (MeV)	a (fm)	r_e (fm)
1	6	17.9 (2.8)	-1.57 (0.10)	0.532 (0.018)
	7	16.2 (3.6)	-1.63 (0.15)	0.538 (0.023)
	8	14.6 (5.8)	-1.69 (0.26)	0.537 (0.035)
	9	24.5 (11.5)	-1.35 (0.28)	0.468 (0.049)
	10	46.9 (20.7)	-1.04 (0.20)	0.407 (0.075)
	11	38.3 (31.4)	-1.18 (0.35)	0.473 (0.142)
2	6	18.3 (3.0)	-1.43 (0.15)	0.532 (0.022)
	7	16.4 (3.9)	-1.53 (0.19)	0.541 (0.031)
	8	15.3 (6.0)	-1.57 (0.23)	0.556 (0.044)
	9	25.0 (11.7)	-1.27 (0.29)	0.497 (0.059)
	10	46.3 (20.7)	-1.08 (0.17)	0.412 (0.082)
	11	39.1 (31.4)	-1.18 (0.33)	0.468 (0.135)

5. Summary and concluding remark

We study the $N\Omega$ interaction in the ${}^5S_2$ channel through the equal-time NBS wave function in (2+1)-flavor lattice QCD simulations on a $(1.92\text{fm})^3 \times 3.84$ fm lattice at the quark masses corresponding to $m_\pi = 875(1)$ MeV and $m_K = 916(1)$ MeV.

We extract the central potential from the NBS wave function for the ${}^5S_2$ channel by using the time-dependent HAL QCD method. The result shows attraction for all distances in this channel. We found that the attraction is strong enough to produce one $N\Omega$ bound state in the spin-2 channel at our quark mass. In our study we obtain $B_{N\Omega} = 18.9(5.0)(^{+12.1}_{-1.8})$ MeV, $a_{N\Omega} = -1.28(0.13)(^{+0.14}_{-0.15})$ fm and $(r_e)_{N\Omega} = 0.499(0.026)(^{+0.029}_{-0.048})$ fm.

Our present study may be considered as a starting point to answer the long standing question about the existence of the $N\Omega$ bound state in the spin-2 channel. We are currently studying the $N\Omega$ potential by using gauge configurations at larger lattice volume with smaller quark masses generated by PACS-CS collaboration[29]. In the near future, large volume simulations at the physical quark masses using K-computer at RIKEN AICS [30] with the coupled-channel HAL QCD method would make a final conclusion on the fate of the $N\Omega$ bound state.

Acknowledgment

We thank CP-PACS/JLQCD Collaborations and ILDG/JLDG for providing us the 2+1 flavor gauge configurations. We are grateful for the authors and maintainers of Bridge++[31], a modified version of which is used for calculations in this work. T.H. would like to express his sincere thanks to the late Prof. Gerry Brown who gave him kind and constant encouragement for many years. F.E. thanks Prof. M. M. Firoozabadi for his support. He is also supported in part by Department of Physics Bilateral International Exchange Program (BIEP) 2013, Kyoto University, and thanks Yukawa Institute for Theoretical Physics, Kyoto University for a kind hospitality during his stay while completing this paper. This research is supported in part by Grant-in-Aid for Scientific Research on Innovative Areas(No.2004:20105001, 20105003) and for Scientific Research (B) 25287046, 24740146, (C) 23540321 and SPIRE (Strategic Program for Innovative Research). T.H. is partially supported by RIKEN iTHES project.

References

[1] R.L. Jaffe, Phys. Rev. Lett. **38** (1977) 195.

[2] J. T. Goldman, K. Maltman, G. J. Stephenson, Jr., K. E. Schmidt and F. Wang, Phys. Rev. Lett. **59**, 627 (1987).

[3] M. Oka, Phys. Rev. D **38**, 298 (1988).

[4] A. Gal, in *From Nuclei to Stars, Festschrift in Honor of Gerald E. Brown*, Ed. Sabine Lee (World Scientific, 2011) pp. 157-170 [arXiv:1011.6322 [nucl-th]].

[5] M. Lüscher, Nucl. Phys. B **354**, 531 (1991).

[6] N. Ishii, S. Aoki and T. Hatsuda, Phys. Rev. Lett. **99** (2007) 022001.

[7] S. Aoki, T. Hatsuda and N. Ishii, Comput. Sci. Dis. **1**, 015009 (2008) [arXiv:0805.2462 [hep-ph]].

[8] S. Aoki, T. Hatsuda and N. Ishii, Prog. Theor. Phys. **123** (2010) 89.

[9] N. Ishii *et al.* [HAL QCD Collaboration], Phys. Lett. B **712** (2012) 437.

[10] S. Aoki *et al.* [HAL QCD Collaboration], PTEP **2012** (2012) 01A105.

[11] T. Inoue *et al.* [HAL QCD Collaboration], Prog. Theor. Phys. **124** (2010) 591 [arXiv:1007.3559 [hep-lat]].

[12] S. R. Beane *et al.* [NPLQCD Collaboration], Phys. Rev. Lett. **106** (2011) 162001 [arXiv:1012.3812 [hep-lat]].

[13] T. Inoue *et al.* [HAL QCD Collaboration], Phys. Rev. Lett. **106** (2011) 162002 [arXiv:1012.5928 [hep-lat]].

[14] T. Inoue *et al.* [HAL QCD Collaboration], Nucl. Phys. A **881** (2012) 28 [arXiv:1112.5926 [hep-lat]].

[15] S.R. Beane, E. Chang, W. Detmold, B. Joo, H.W. Lin, T.C. Luu, K. Orginos and A. Parreno *et al.*, Mod. Phys. Lett. A 26 (2011) 2587 [arXiv:1103.2821 [hep-lat]].

[16] P.E. Shanahan, A.W. Thomas and R.D. Young, Phys. Rev. Lett. 107 (2011) 092004 [arXiv:1106.2851 [nucl-th]]; arXiv:1308.1748 [nucl-th].

[17] F. Wang et al., Phys. Rev. C **51**, 3411 (1995) [nucl-th/9512014];
H. -r. Pang et al., Phys. Rev. C **69**, 065207 (2004) [nucl-th/0306043];
M. Chen et al., Phys. Rev. C **83**, 015202 (2011).

[18] Q. B. Li and P. N. Shen, Eur. Phys. J. A **8**, 417 (2000) [nucl-th/9910060]; Q. B. Li et al., Nucl. Phys. A **683**, 487 (2001) [nucl-th/0009038]; D. Zhang et al., Phys. Rev. C **75**, 024001 (2007) [nucl-th/0609008].

[19] R. Tamagaki and W. Watari, Prog. Theor. Phys. Suppl. 39, 23 (1967).

[20] C. J. D. Lin, G. Martinelli, C. T. Sachrajda and M. Testa, Nucl. Phys. B **619**, 467 (2001).

[21] S. Aoki *et al.* [CP-PACS Collaboration], Phys. Rev. D **71**, 094504 (2005).

[22] N. Ishizuka, PoS **LAT2009**, 119 (2009).

[23] S. Aoki, N. Ishii, T. Doi, Y. Ikeda and T. Inoue, Phys. Rev. D **88**, 014036 (2013) [arXiv:1303.2210 [hep-lat]].

[24] CP-PACS and JLQCD Collaborations, http://www.jldg.org/ildg-data/CPPACS+JLQCDconfig.html.

[25] T. Ishikawa *et al.* [CP-PACS and JLQCD Collaborations], Phys. Rev. D **78**, 011502 (2008) [arXiv:0704.1937 [hep-lat]].

[26] S. Aoki *et al.* [HAL QCD Collaboration], Proc. Japan Acad. B **87**, 509 (2011) [arXiv:1106.2281 [hep-lat]].

[27] S. Aoki, B. Charron, T. Doi, T. Hatsuda, T. Inoue and N. Ishii, Phys. Rev. D **87**, no. 3, 034512 (2013) [arXiv:1212.4896 [hep-lat]].

[28] K. Sasaki, Few Body Syst. **54**, 1109 (2013).

[29] S. Aoki *et al.* [PACS-CS Collaboration], "2+1 Flavor Lattice QCD toward the Physical Point," Phys. Rev. D **79**, 034503 (2009) [arXiv:0807.1661 [hep-lat]].

[30] S. Aoki *et al.* [PACS-CS Collaboration], PTEP **2012**, 01A102 (2012).

[31] http://bridge.kek.jp/Lattice -code/docs/html.1.0.5.